



UN-SiC TRISO Post Irradiation Examination Developmental Work

July 2024

Changing the World's Energy Future

Karen E Wright, Robert O Hoover



INL is a U.S. Department of Energy National Laboratory operated by Battelle Energy Alliance, LLC

DISCLAIMER

This information was prepared as an account of work sponsored by an agency of the U.S. Government. Neither the U.S. Government nor any agency thereof, nor any of their employees, makes any warranty, expressed or implied, or assumes any legal liability or responsibility for the accuracy, completeness, or usefulness, of any information, apparatus, product, or process disclosed, or represents that its use would not infringe privately owned rights. References herein to any specific commercial product, process, or service by trade name, trade mark, manufacturer, or otherwise, does not necessarily constitute or imply its endorsement, recommendation, or favoring by the U.S. Government or any agency thereof. The views and opinions of authors expressed herein do not necessarily state or reflect those of the U.S. Government or any agency thereof.

UN-SiC TRISO Post Irradiation Examination Developmental Work

Karen E Wright, Robert O Hoover

July 2024

**Idaho National Laboratory
Idaho Falls, Idaho 83415**

<http://www.inl.gov>

**Prepared for the
U.S. Department of Energy
Under DOE Idaho Operations Office
Contract DE-AC07-05ID14517**



UN-SiC TRISO Post Irradiation Examination Developmental Work

July 2024

Karen E Wright and Robert Hoover
Idaho National Laboratory



*INL is a U.S. Department of Energy National Laboratory
operated by Battelle Energy Alliance, LLC*

DISCLAIMER

This information was prepared as an account of work sponsored by an agency of the U.S. Government. Neither the U.S. Government nor any agency thereof, nor any of their employees, makes any warranty, expressed or implied, or assumes any legal liability or responsibility for the accuracy, completeness, or usefulness, of any information, apparatus, product, or process disclosed, or represents that its use would not infringe privately owned rights. References herein to any specific commercial product, process, or service by trade name, trade mark, manufacturer, or otherwise, does not necessarily constitute or imply its endorsement, recommendation, or favoring by the U.S. Government or any agency thereof. The views and opinions of authors expressed herein do not necessarily state or reflect those of the U.S. Government or any agency thereof.

UN-SiC TRISO Post Irradiation Examination Developmental Work

Karen E Wright and Robert Hoover
Idaho National Laboratory

July 2024

Idaho National Laboratory
Advanced Reactor Technologies
Idaho Falls, Idaho 83415

<http://www.art.inl.gov>

Prepared for the
U.S. Department of Energy
Office of Environmental Management
Under DOE Idaho Operations Office
Contract DE-AC07-05ID14517

Page intentionally left blank

INL ART Program

**UN-SiC TRISO Post Irradiation Examination
Developmental Work**

INL/RPT-24-78550
Revision 1

July 2024

Technical Reviewer: (Confirmation of mathematical accuracy, and correctness of data and appropriateness of assumptions.)



Paul A. Demkowicz
INL ART TRISO Fuel Director

7/17/2024

Date

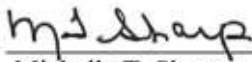
Approved by:



Travis R. Mitchell
INL ART Project Manager

7/19/2024

Date



Michelle T. Sharp
INL Quality Assurance

7/15/2024

Date

Page intentionally left blank

SUMMARY

As part of efforts to strengthen INL's capabilities in post-irradiation analysis of non-Advanced Gas Reactor (AGR) tristructural isotropic (TRISO) fuels, two developmental activities were conducted. The first was to determine how best to analyze uranium nitride TRISO fuel kernels using electron-probe microanalysis (EMPA), while the second focused on developing a method to deconsolidate TRISO fuel particles that have been encased in a silicon carbide matrix. Because these two activities were unrelated, they have been presented separately in this report.

Initial EPMA analyses showed nitrogen contents that far exceeded the concentration expected for UN, a line compound. Further examination showed that current literature values for the mass absorption coefficient (MAC) for the N $K\alpha$ X-ray absorbed by U ranged from approximately 1600 to 9500, with most values tending toward 9500. Measuring UN with five different progressively increasing accelerating voltages followed by analysis using the modeling program xMAC suggests the actual MAC is approximately 2115. Additional MAC modifications were required to produce reasonable analytical results.

Because of the inaccuracies of necessary MAC coefficients, UN analysis via scanning electron microscopy (SEM) is likely to produce inaccurate results. This is because SEM software does not typically allow the user to alter MACs.

Tests have been performed to examine the feasibility of an electrochemical technique to liberate irradiated TRISO fuel from a SiC matrix without damaging the outer pyrolytic carbon layer of the fuel particle. The method is performed by electrochemically exposing the SiC to magnesium metal forming Mg_2Si and C. Following exposure, the small SiC samples showed slight mass increases with no evidence of conversion to Mg_2Si and C nor obvious degradation of the SiC samples.

Page intentionally left blank

CONTENTS

SUMMARY	vii
ACRONYMS.....	xi
1. PART 1: UN ELECTRON PROBE MICROANALYSIS	1
1.1 Introduction for UN Electron Probe Microanalysis	1
1.2 EPMA Methods.....	1
1.3 Results.....	1
1.4 Conclusions.....	4
2. PART 2: ELECTROCHEMICAL SILICON CARBIDE MATRIX DECONSOLIDATION STUDIES	4
2.1 Introduction for Silicon Carbide Matrix Deconsolidation Studies.....	4
2.2 Electrochemical Deconsolidation.....	5
2.3 Experimental	6
2.3.1 Experimental Setup	6
2.3.2 Molten Salt Characterization	7
2.3.3 Mg Reduction onto SiC Sample.....	8
2.4 Summary/Recommended Next Steps.....	11
3. REFERENCES.....	11

FIGURES

Figure 1. Measured point locations on a backscatter electron (BSE) UN image.....	2
Figure 2. Schematic of a TRISO fuel particle [4].	4
Figure 3. Photos of the CVD SiC-coated graphite plate before (left) and after (right) the EMS-CC process [4].....	5
Figure 4. Alumina crucible containing LiCl-KCl-MgCl ₂ salt in front of the furnace used for testing of the EMS-CC process.....	6
Figure 5. SiC samples in a stainless-steel mesh basket (left) and hung from a stainless-steel wire (right).	7
Figure 6. Diagram of the experimental setup used to test the EMS-CC process.	7
Figure 7. Cyclic voltammograms in the LiCl-KCl-MgCl ₂ salt at ~500°C.....	8
Figure 8. SiC sample A after removal from the furnace.	9
Figure 9. SiC sample B with stainless-steel wire lead.	10
Figure 10. SiC sample B with stainless-steel wire lead.	10

TABLES

Table 1. Example UN point analysis.	1
Table 2. Reanalysis of point from Table 1 using modified MACs.	2
Table 3. Reanalysis of point from Table 1 and Table 2 using additional modified MACs.	2
Table 4. Reanalysis of point from Table 1 and Table 2 using additional modified MACs and replacing the metallic U standard with UO ₂	2
Table 5. Point analysis results in wt.% for locations shown in Figure 1.	3
Table 6. Point analysis results in at. % for locations shown in Figure 1.	3
Table 7. ORNL wt% analysis of particles from the same lot as those used in this study.	3
Table 8. ORNL at% analysis of particles from the same lot as those used in this study.	3
Table 9. Summary of gravimetric data.....	11

ACRONYMS

ATR	Advanced Test Reactor
BSE	Back scattered electron
CV	Cyclic voltammetry
CVD	Chemical vapor deposition
EMS-CC	Electrolytic Molten Salt Carbon Conversion
EPMA	Electron Probe Microanalysis
INL	Idaho National Laboratory
MAC	Mass absorption coefficient
NIST	National Institute of Standards and Technology
ORNL	Oak Ridge National Laboratory
PIE	Post-irradiation examination
SEM	Scanning electron microscopy
TRISO	Tristructural isotropic
XRD	X-ray diffraction
Z	Atomic number
ΔG	Change in Gibbs free energy

Page intentionally left blank

UN-SiC TRISO Post Irradiation Examination Developmental Work

1. PART 1: UN ELECTRON PROBE MICROANALYSIS

1.1 Introduction for UN Electron Probe Microanalysis

Electron probe microanalysis (EPMA) of nuclear fuels is often difficult due to a paucity of accurate fundamental properties such as mass absorption coefficients (MACs), which are essential to accurate EPMA quantification.

Because Idaho National Laboratory (INL) will need to perform post irradiation examination on irradiated UN TRISO fuel particles, it is necessary to study non-irradiated UN kernels to determine the best approach for EPMA analysis.

This work has several objectives:

1. To determine UN sample homogeneity
2. To determine what analytical standards should be employed
3. To determine whether the EPMA can analyze these materials accurately.

1.2 EPMA Methods

Oak Ridge National Laboratory (ORNL) provided INL with approximately one gram of naturally enriched UN kernels with diameters ranging from 380 to 400 μm . Numerous particles were mounted into miniature metallography mounts and epoxied in place. They were then polished with diamond slurry to a surface finish of approximately 0.5 μm . Following polishing, the miniature mounts were coated with 10 nm of Ir to ensure sample conductivity and were loaded into a Cameca SX100-R EPMA for analysis.

Ideally, calibration standards should be matrix-matched to the sample being measured; however, such standards were not available. Instead, calibration standards U metal, UO_2 , BN and SiC were selected and then elements U, C, N, and O were calibrated using a 20 keV accelerating voltage.

1.3 Results

Initial results using the PAP [1] matrix correction program and MACs that were a combination of Pouchou and Pichoir MACs [1] for light elements and Farthing and Walker MACs [2] for heavy elements yielded the following example point analysis (Table 1). Note that O analysis was not included because the O appeared to result from surface adsorption rather than as a UN component.

Table 1. Example UN point analysis.

U wt%	N wt%	C wt%	Analytical Total (%)
103.2	17.7	2.56	123.5

Both U and N show much higher concentrations than expected, or indeed, even feasible given the analytical total is $\gg 100\%$. Because the EPMA quantification software has several MAC databases from which to choose, it is possible to view the range of previously determined MACs. The MAC for N $\text{K}\alpha$ X-ray in U in these databases ranges from 1598 to 9501, indicating considerable disagreement. For light-heavy element pairs with known composition, it is possible to use a multivoltage analytical technique to compute the MAC of the light element by the heavy element [3]. Using the provided UN samples, the N $\text{K}\alpha$ X-ray in U MAC was estimated to be 2115, with a U $\text{M}\alpha$ X-ray self-absorption MAC of 609.

Using these new MAC coefficients, analysis of the same spot in Table 1 yielded the following (Table 2):

Table 2. Reanalysis of point from Table 1 using modified MACs.

U wt%	N wt%	C wt%	Analytical Total (%)
100.4	5.85	2.59	108.9

While the above analysis is improved, the analytical total remains $\gg 100\%$. General EPMA practice from non-irradiated material expects analytical total ranges from 98 to 102%. Ultimately National Institute of Standards and Technology (NIST)-provided MACs for C ka in U, N ka in C, and C ka in N were employed, with the following result (Table 3):

Table 3. Reanalysis of point from Table 1 and Table 2 using additional modified MACs.

U wt%	N wt%	C wt%	Analytical Total (%)
99.6	5.15	0.99	105.8

Finally, the U-metal analytical calibration standard was replaced by UO_2 , with the following result (Table 4).

Table 4. Reanalysis of point from Table 1 and Table 2 using additional modified MACs and replacing the metallic U standard with UO_2 .

U wt%	N wt%	C wt%	Analytical Total (%)
96.3	5.20	1.02	102.5

Figure 1 shows the location of five measured points with results shown in Table 5 (weight %) and Table 6 (atomic %).

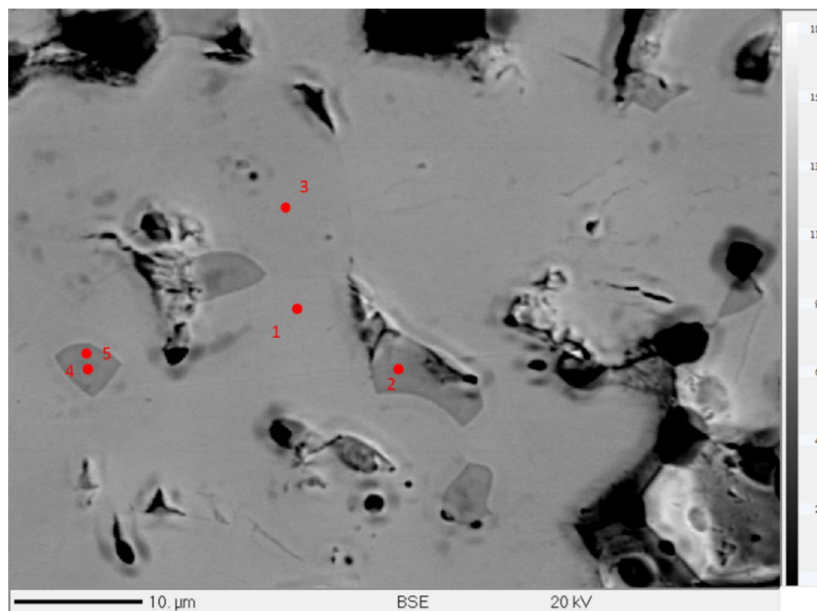


Figure 1. Measured point locations on a backscatter electron (BSE) UN image.

Table 5. Point analysis results in wt.% for locations shown in Figure 1.

±	1.1	0.08	0.04	
	U wt%	N wt%	C wt%	Total
Spot 1	96.3	5.20	1.02	102.5
Spot 2	86.4	3.81	<0.02	90.2
Spot 3	96.7	5.21	0.99	102.9
Spot 4	86.0	3.59	<0.02	89.6
Spot 5	88.1	3.74	0.03	91.9

Table 6. Point analysis results in at. % for locations shown in Figure 1.

	U at%	N at%	C at%
Spot 1	47.0	43.1	9.88
Spot 2	57.2	42.8	0
Spot 3	47.2	43.2	9.60
Spot 4	58.5	41.5	0
Spot 5	57.8	41.7	0.45

While Spot Locations 1 and 3 (Figure 1) show slightly elevated analytical totals, Spot Locations 2, 4, and 5 are quite low. Because the grayscale in the BSE for these locations is darker than the surrounding area, this suggests that the proportion of low-atomic number (Z) elements in these locations is higher than in Spot Locations 1 and 3. Additionally, low analytical totals often suggest that an element present in the sample has not been included in the analysis. However, attempts to identify a candidate “missing” element failed to find any unidentified peaks in the spectrum. While the reason for the low analytical totals for those spots remains uncertain, it is possible that those locations represent pores with a very thin UN layer over the top. Such a geometrical arrangement could account for these observations.

ORNL provided an analysis of particles from the same lot from which these particles were obtained. They used inductively coupled plasma mass spectroscopy to measure the U concentration and infrared absorption using a LECO instrument to quantify O, N, and C. Results are shown in Table 7 and Table 8.

Table 7. ORNL wt% analysis of particles from the same lot as those used in this study.

±		0.11	0.09	0.04	
	U wt%	N wt%	C wt%	O wt%	Total
	95.01	4.480	0.902	0.005	100.397

Table 8. ORNL at% analysis of particles from the same lot as those used in this study.

U at%	N at%	C at%	O at%
50.23	40.27	9.46	0.039

In comparing EPMA weight-percent analysis of Spots 1 and 3 (Table 5 and Table 6) performed at INL with ORNL’s weight-percent analysis of other particles from the same lot, it is evident that the U and C analyses are nearly or within measurement error for the two techniques, while the EPMA N analysis is approximately 16% higher than ORNL’s analysis. Assuming ORNL’s N analysis is more accurate than INL’s EPMA N analysis suggests that additional efforts are necessary to constrain the N MAC. If the oxygen analysis provided by ORNL is accurate, EPMA cannot detect oxygen at that concentration using the described techniques.

Because accurate analysis with microanalysis techniques such as EPMA and scanning electron microscopy (SEM) rely on analyzing the majority (i.e., at least 98%) of mass present, the lack of accurate MACs for this system will negatively impact SEM analysis. This is because SEM software typically does not permit the user to alter the MACs or to change the matrix-correction algorithm.

1.4 Conclusions

This section of the summary reaches the following conclusions:

1. EPMA analysis of unirradiated UN kernels suggests that numerous MACs are incorrect and require modification.
2. Kernels appear homogeneous on a whole-kernel scale. Apparent heterogeneities on a smaller scale may represent pores with a thin veneer of UN covering them.
3. EPMA-measured N concentrations appear to be elevated beyond their expected value. Additional investigation to better constrain the N MAC is warranted.
4. The lack of accurate MACs will negatively impact SEM analysis as neither MACs nor matrix correction procedures can be altered by the user.
5. Because the particles are relatively homogeneous, they can be used as an EPMA analytical standard, greatly improving EPMA accuracy for these materials.

2. PART 2: ELECTROCHEMICAL SILICON CARBIDE MATRIX DECONSOLIDATION STUDIES

2.1 Introduction for Silicon Carbide Matrix Deconsolidation Studies

TRISO fuels, developed for use in high temperature gas cooled reactors, consists of a small (~0.5 mm) fuel kernel surrounded by layers of silicon carbide and carbon (Figure 2). These small pebbles (<1 mm) are commonly embedded in a matrix of graphite. Several different commercial entities are currently exploring the use of SiC as a matrix rather than graphite as was used for the AGR program. Identifying methods to deconsolidate the SiC matrix from the fuel particles will aid with post irradiation examination.



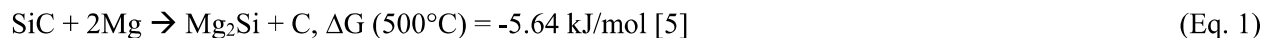
Figure 2. Schematic of a TRISO fuel particle [4].

To facilitate expanded post-irradiation examination (PIE) of the fuel, the fuel kernels must be extracted from the SiC matrix without damaging the fuel particles themselves. The purpose of the work

presented in this document is to examine the feasibility of an electrochemical technique to deconsolidate the SiC matrix from the irradiated fuel.

2.2 Electrochemical Deconsolidation

Previous work in Korea by Lee et al. [4] looked at methods for treating spent TRISO fuel. As part of this study, the researchers demonstrated an electrolytic molten-salt carbon-conversion (EMS-CC) process for breaching the SiC layer of a TRISO particle. This technique involves electrochemically depositing magnesium metal (Mg), below its melting point (648°C), from a molten salt onto the SiC surface. The magnesium reacts with the SiC to form magnesium silicide (Mg₂Si) and carbon (C) (Equation 1).



where ΔG represents the change in Gibbs free energy.

As carbon is a product of the desired reaction (Equation 1), the Mg is not expected to react with the outer pyrolytic carbon layer of the TRISO particle and should not damage the particle itself.

In this published work, researchers deposited Mg onto a ~30 μm thick SiC-coated (by chemical vapor deposition [CVD]) graphite plate. The Mg was reduced from a molten salt consisting of a LiCl-KCl eutectic salt containing 5.7 wt% MgCl₂ at 500°C. The charge passed was equivalent to 0.52 g of Mg. Photos of the CVD SiC-coated graphite plate, both before (left) and after (right) the reaction are shown in Figure 3. Following the reaction, the researchers used X-ray diffraction (XRD) in the reaction zone and detected SiC, Mg, and Mg₂Si, demonstrating that the EMS-CC reaction occurred. After rinsing, only SiC was detected in the reaction zone.

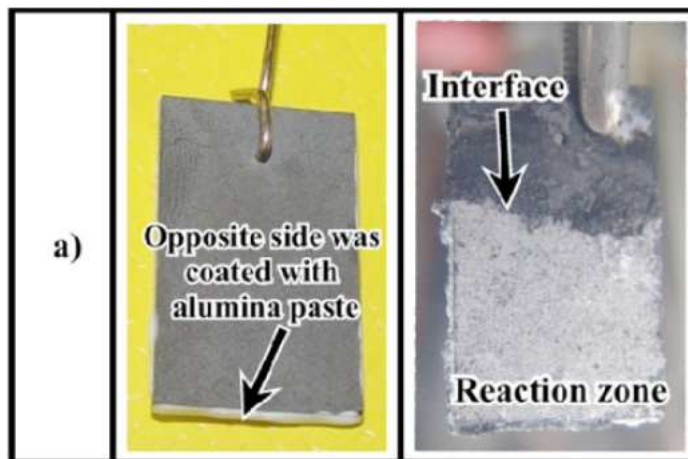


Figure 3. Photos of the CVD SiC-coated graphite plate before (left) and after (right) the EMS-CC process [4].

Based on the apparent success of the EMS-CC process, this technique was tested at INL to deconsolidate larger pieces of pure SiC.

2.3 Experimental

2.3.1 Experimental Setup

The EMS-CC experiments were performed using a molten-salt furnace in an argon-atmosphere glovebox. The atmosphere was maintained below 10 ppm H_2O and O_2 throughout the duration of the tests. An alumina crucible was loaded with 188 g LiCl-KCl eutectic (58.5 mol% LiCl, 41.5 mol% KCl) salt (Aldrich, 99.99%) and 12 g MgCl_2 (ThermoFisher, 99.99%). The alumina crucible containing the salt is seen in Figure 4 in front of the molten-salt furnace in the argon glovebox. The cathode consisted of a densified SiC sample provided by ORNL. These samples are nominally composed of 50–60 vol% alpha-phase SiC particles bonded together by a beta-phase SiC matrix. The samples were densified to ~90% theoretical density. The SiC samples, ~12 mm in diameter and 4 mm thick, were either placed in a stainless-steel mesh basket (Figure 5, left) or hung from a stainless-steel wire through a small hole drilled into the SiC sample (Figure 5, right). Additionally, a 1 mm tantalum wire (ThermoFisher, 99.95%) was used as an anode along with a Ag/AgCl reference electrode. A schematic of the setup is shown in Figure 6.



Figure 4. Alumina crucible containing LiCl-KCl- MgCl_2 salt in front of the furnace used for testing of the EMS-CC process.

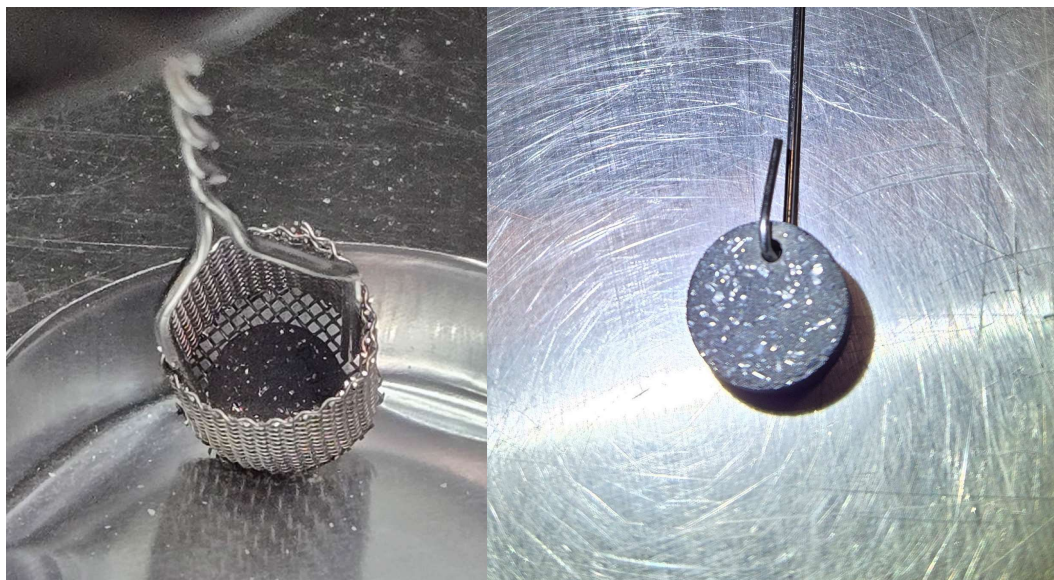


Figure 5. SiC samples in a stainless-steel mesh basket (left) and hung from a stainless-steel wire (right).

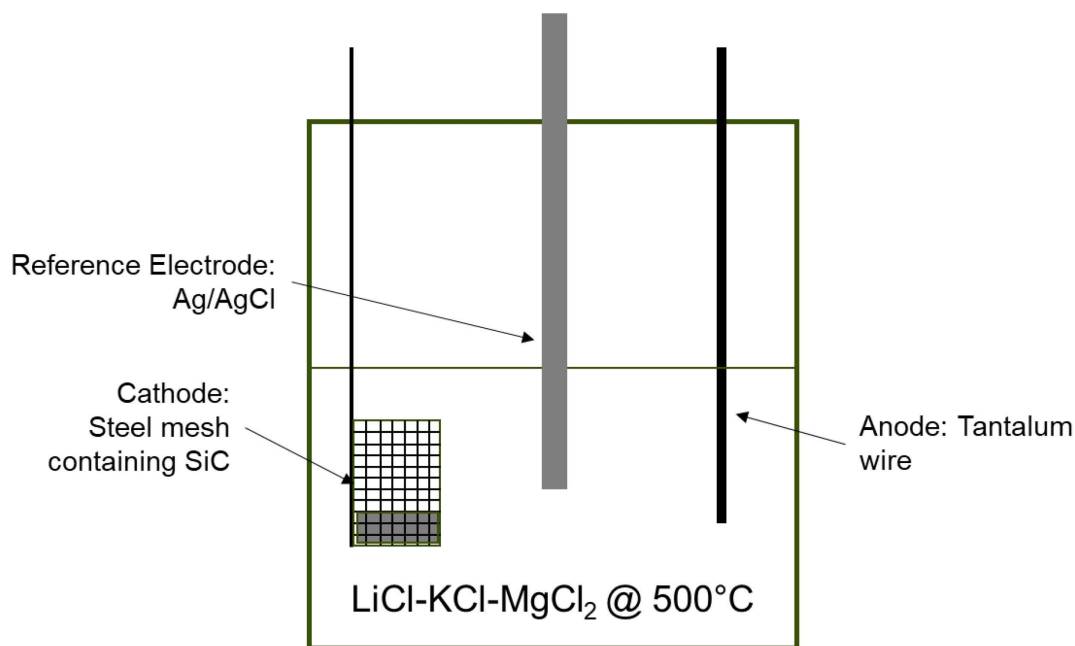


Figure 6. Diagram of the experimental setup used to test the EMS-CC process.

2.3.2 Molten-Salt Characterization

Cyclic voltammetry (CV) was performed in the LiCl-KCl-MgCl_2 salt to characterize the salt and to determine the potential at which Mg is reduced and deposited onto the cathode/SiC sample. CVs were collected in the salt at $\sim 500^\circ\text{C}$ with a tantalum wire working electrode, stainless-steel mesh basket counter electrode, and Ag/AgCl reference electrode. CVs were collected at a scan rate of 100 mV/s, with varying vertex potentials as shown in Figure 7. Reduction of Mg^{2+} to Mg appears to occur at approximately -1.77 V vs Ag/AgCl.

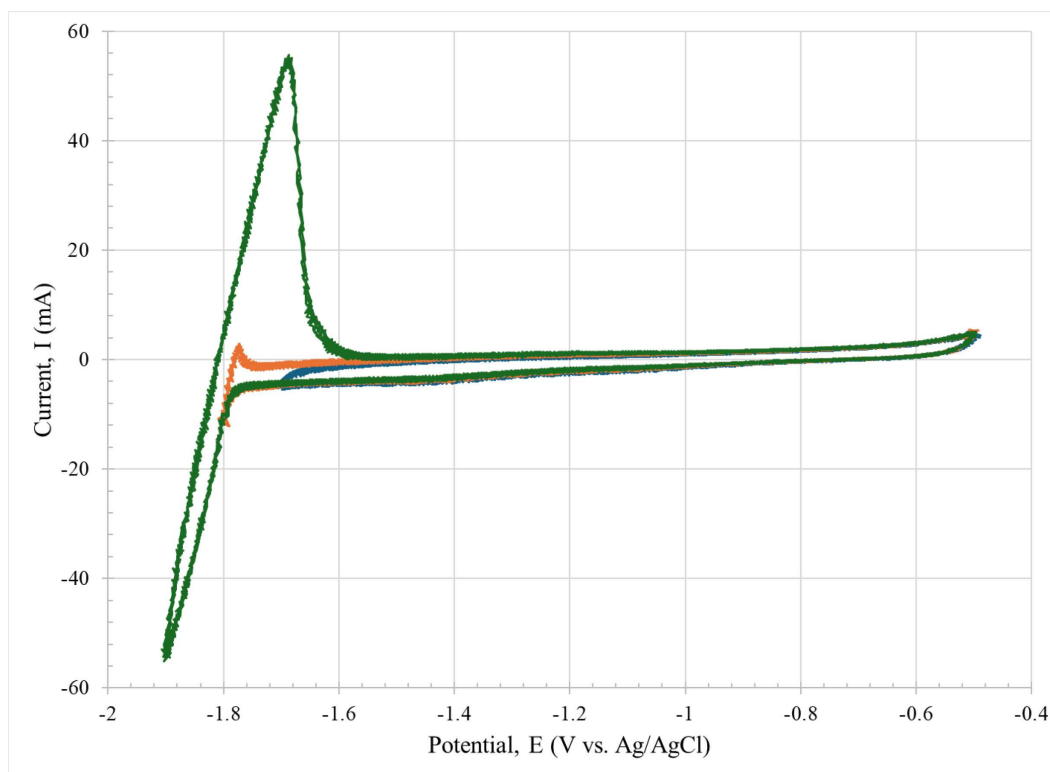


Figure 7. Cyclic voltammograms in the LiCl-KCl-MgCl₂ salt at ~500°C.

2.3.3 Mg Reduction onto SiC Sample

2.3.3.1 Tests 1 and 2: Mesh Basket

SiC sample A was weighed (1.4711 g), loaded into the steel mesh basket, and lowered into the molten salt. A cathodic potential of -1.80 to -1.90 V was applied to reduce and to deposit Mg onto the SiC sample, resulting in a current on the order of 100 mA. After applying the cathodic potential, the sample was kept in the furnace at temperature overnight to allow time for the reaction described in Equation 1 to proceed. After the overnight period, any remaining magnesium metal was electrolytically stripped away from the cathode to the tantalum-anode wire. A total net charge of 897 coulombs was passed, which is equivalent to ~113 mg magnesium. According to the reaction stoichiometry, this should equate to 93 mg of SiC converting into Mg₂Si. Following removal from the salt, the basket and sample were rinsed with water to remove the salt, dried at room temperature, and weighed. The final SiC sample mass was 1.4947 g, or a mass gain of 23.6 mg (Table 9). A photo of the SiC sample after removal from the furnace and before rinsing is shown in Figure 8.



Figure 8. SiC sample A after removal from the furnace.

SiC sample A was used again for Test 2. The sample was weighed, loaded into the steel mesh basket, and lowered into the salt. Similar cathodic potentials were applied and the sample was kept at temperature in the furnace overnight, followed by the stripping of any remaining magnesium from the basket. A total net charge of 698 coulombs was passed, which would be equivalent to ~88 mg magnesium and would equate to 73 mg SiC converting to Mg_2Si . The sample was removed, rinsed, dried, and weighed. The final mass of the SiC sample was 1.4876 g, or a mass loss of 7.1 mg for Test 2 and an overall mass gain of 16.5 mg over the two tests (Table 9).

2.3.3.2 Test 3: Hanging Sample

In using the stainless-steel mesh basket to submerge the sample into the salt, the majority of the surface area for Mg to deposit is the mesh basket itself and not the SiC sample. To increase the portion of the Mg deposited directly in contact with the sample, the method of submerging and providing electric contact to the sample was changed for Test 3. A small (1/16-in.) hole was drilled into Sample B and a stainless-steel wire was used to hang the sample into the salt, as shown in Figure 9.

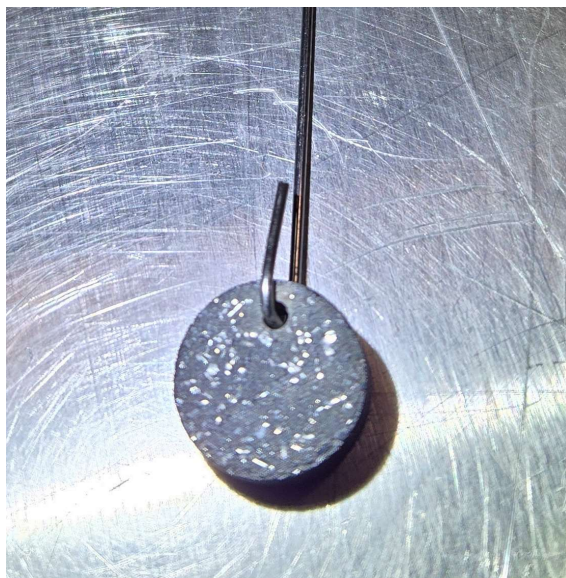


Figure 9. SiC sample B with stainless-steel wire lead.

As with the first two tests, Mg was reduced and deposited onto the SiC sample at -1.80 to -1.90 V with average current on the order of 100 mA. The sample remained in the furnace at temperature overnight to allow the reaction to proceed, after which any remaining magnesium was electrolytically stripped away. A total net charge of 999 coulombs, equivalent to 126 mg magnesium, was passed which equates to the conversion of 104 mg SiC into Mg_2Si . The sample was then removed from the furnace, rinsed, dried, and weighed, giving a mass of 1.4684 g, or a slight increase from the original mass. After the initial rinse and room temperature dry, the sample was soaked overnight in water and dried at 250°C for approximately 2 hours to see if any additional salt and/or water could be removed. Following the soak and higher-temperature dry, the mass decreased slightly to 1.455 g (Table 9). A photo of the SiC sample after removal from the furnace and before rinsing can be seen in Figure 10.



Figure 10. SiC sample B with stainless-steel wire lead.

Table 9. Summary of gravimetric data.

Test	Sample	Initial Mass	Theoretical (based on charge passed and full reaction)			Experimental Results
			Mg Reduced	SiC Reacted	Final SiC Mass	Final SiC Mass
1	A (basket)	1.4711 g	113 mg	93 mg	1.378 g	1.4947 g
2	A (basket)	1.4947 g	88 mg	73 mg	1.422 g	1.4876 g
3	B (hang)	1.4394 g	126 mg	104 mg	1.336 g	1.4684 g (post-rinse) 1.455 g (post-soak)

Note: Tolerance of balance is ± 1.8 mg.

2.4 Summary/Recommended Next Steps

Overall, the tests showed slight increases in the SiC sample mass following contact with electrolytically produced magnesium metal using the Electrolytic Molten Salt Carbon Conversion (EMS-CC) process. It was expected that, if successful, the process would result in a mass decrease as SiC was converted to Mg_2Si and C, which would then be rinsed away. From this observation, along with no visual indication of SiC degradation or change, there was no clear sign of SiC deconsolidation.

Good contact/interaction between the SiC and magnesium metal is thought to be essential for this reaction to occur. Future work should include direct contact between the SiC sample and molten magnesium metal. Magnesium metal has a melting point of 650°C , necessitating an experimental temperature of $\sim 700^\circ\text{C}$. It should be noted that at this increased temperature, the reaction (Equation 1) is slightly less favorable with $\Delta G = -4.44$ kJ/mol, compared with $\Delta G = -5.64$ kJ/mol at 500°C [5].

3. REFERENCES

1. Pouchou, J. L., and F. Pichoir. 1991. *Quantitative Analysis of Homogeneous or Stratified Microvolumes Applying the Model "PAP"* K. F. J. Heinrich and D. E. Newbury (eds.), Electron Probe Quantification, New York, Plenum Press, 31-76. https://doi.org/10.1007/978-1-4899-2617-3_4.
2. Farthing, I. R., and C. T. Walker. 1990. "Heinrich's Mass Absorption Coefficients for the K, L, and M Lines," The European Commission, Institute for Transuranium Elements, Karlsruhe, Report K0290140.
3. Pouchou, J. L. 2013. xMAC v. 4.0.
4. Lee, J. H., et al. 2008. "A Feasibility Study for the Development of Alternative Methods to Treat a Spent TRISO Fuel." *Nuclear Technology* 162(2): 250–258. <https://doi.org/10.13182/NT08-A3953>.
5. HSC Chemistry, HSC Reaction Module, Version 9.8.1.2, Outokumpu Research, 2018.